Nuclear Medicine and Biology 96 (2021) 68–79

Contents lists available at ScienceDirect

Nuclear Medicine and Biology

journal homepage: www.elsevier.com/locate/nucmedbio

Investigating intrinsic radiosensitivity biomarkers to peptide receptor radionuclide therapy with [^{177}Lu]Lu-DOTATATE in a panel of cancer cell lines

Wendy Delbart [a,b,*], Ghanem E. Ghanem [a,b], Ioannis Karfis [a], Patrick Flamen [a], Zéna Wimana [a,b]

[a] Nuclear Medicine Department, Institut Jules Bordet, Université Libre de Bruxelles (ULB), Brussels, Belgium
[b] Laboratory of Oncology and Experimental Surgery, Institut Jules Bordet, Université Libre de Bruxelles (ULB), Brussels, Belgium

ARTICLE INFO

Article history:
Received 28 December 2020
Received in revised form 2 March 2021
Accepted 20 March 2021
Available online xxxx

Keywords:
Peptide receptor radionuclide therapy
[^{177}Lu]Lu-DOTATATE
Radiosensitivity
Oxidative stress

ABSTRACT

Introduction: [^{177}Lu]Lu-DOTATATE is an effective systemic targeted radionuclide therapy for somatostatin receptor (SSTR) positive metastatic or inoperable neuroendocrine tumours (NET). However, for a given injected activity, tumour responses are variable. Our aim was to investigate whether SSTR expression/functionality and known characteristics of intrinsic radiosensitivity, namely proliferation rate, glucose metabolism, cell cycle phase, DNA repair and antioxidant defences were predictors of sensitivity to [^{177}Lu]Lu-DOTATATE in SSTR expressing human cancer cell lines.

Methods: In six human cancer cell lines and under basal condition, SSTR expression was assessed by qRT-PCR and immunocytochemistry. Its functionality was evaluated by binding/uptake assays with [^{68}Ga]Ga- and [^{177}Lu]Lu-DOTATATE. The radiosensitivity parameters were evaluated as follows: proliferation rate (cell counting), glucose metabolism ([^{18}F]FDG uptake), antioxidant defences (qRT-PCR, colorimetric assay, flow cytometry), DNA repair (qRT-PCR) and cell cycle (flow cytometry). Effect of [^{177}Lu]Lu-DOTATATE on cell viability was assessed 3, 7 and 10 days after 4 h incubation with [^{177}Lu]Lu-DOTATATE using crystal violet.

Results: Based on cell survival at day 10, cell lines were classified into two groups of sensitivity to [^{177}Lu]Lu-DOTATATE. One group with <20% of survival decrease (−14 to −1%) and one group with >20% of survival decrease (−22 to −33%) compared to the untreated control cell lines. The latter had significantly lower total antioxidant capacity, glutathione (GSH) levels and glucose metabolism ($p < 0.05$) compared to the first group. SSTR ($p = 0.64$), proliferation rate ($p = 0.74$), cell cycle phase ($p = 0.55$), DNA repair ($p > 0.22$), combined catalase and GSH peroxidase expression ($p = 0.42$) and superoxide dismutase (SOD) activity ($p = 0.41$) were not significantly different between the two groups.

Conclusion: Antioxidant defences may be major determinants in [^{177}Lu]Lu-DOTATATE radiosensitivity.

1. Introduction

Peptide receptor radionuclide therapy (PRRT) is an effective systemic targeted therapy employing radiolabeled peptides designed to deliver a therapeutic radiation dose to cancer cells overexpressing specific receptors [1]. The most successful application of PRRT is ^{177}Lutetium-DOTA-[Tyr3]octreotate ([^{177}Lu]Lu-DOTATATE), targeting somatostatin receptor sub-type 2 (SSTR2) [2] in neuroendocrine tumours (NET). Currently standardized treatment protocols are applied based on the NETTER-1 study [3] and [^{177}Lu]Lu-DOTATATE is typically administered in fixed dose of 7.4 GBq, four cycles given eight to twelve weeks apart. However for a given injected activity, tumour responses are variable [4,5], which warrants the search for predictive biomarkers.

[^{177}Lu]Lu-DOTATATE therapy success relies on SSTR expression. The latter, routinely assessed by the uptake of ^{68}Gallium-DOTA-peptides ([^{68}Ga]Ga-DOTA-peptides) on PET/CT images, is a pre-requisite for therapy to ensure the proper delivery of the therapeutic radiotracer in NET lesions. Higher SSTR density would lead to more internalized activity of [^{177}Lu]Lu-DOTATATE in tumour cells and consequently to higher subsequent ionizing radiation (IR)-induced damages.

Beyond SSTR expression, tumour sensitivity to IR from [^{177}Lu]Lu-DOTATATE may also influence the response. Radiosensitivity has been extensively investigated in the context of IR from external beam radiation therapy (EBRT). Studies have highlighted the importance of several key biological factors in the sensitivity to IR, such as DNA repair [6,7], cell cycle phase [8], proliferation rate, glucose metabolism [9,10] and antioxidant defences [11–14]. Their relative importance in PRRT may vary from EBRT as these two radiation-based therapies are characterized by fundamental differences [15]. To explore their importance in PRRT sensitivity, understanding ^{177}Lu radiation biology is essential. ^{177}Lu, being a

* Corresponding author at: Nuclear Medicine Department, Institut Jules Bordet, Université Libre de Bruxelles (ULB), Brussels, Belgium.
E-mail addresses: wendy.delbart@bordet.be (W. Delbart), gghanem@bordet.be (G.E. Ghanem), ioannis.karfis@bordet.be (I. Karfis), patrick.flamen@bordet.be (P. Flamen), zena.wimana@bordet.be (Z. Wimana).

https://doi.org/10.1016/j.nucmedbio.2021.03.006
0969-8051/

beta emitter with low linear energy transfer (LET) radiation, mainly results in indirect effects and consequently the generation of oxidative damages to not only DNA but also to proteins and lipids [16–18] (Fig. 1). Oxidative damages occur only if oxidants such as reactive oxygen species (ROS) can exceed the antioxidant defence mechanisms of the cell, and thus lead to oxidative stress and cell death [19]. Enzymatic and non-enzymatic antioxidants are crucial in detoxifying ROS and consequently prevent oxidative stress.

The present work investigates the relative influence of basal SSTR expression and different intrinsic radiosensitivity factors on the IR effect induced by [^{177}Lu]Lu-DOTATATE in several human cancer cell lines.

2. Material and methods

2.1. Cell lines

The melanoma cell lines (HBL [20–23] and MM162 [24]) were established in our laboratory. Multiple myeloma (COLO-677 and EJM), gastroenteropancreatic (GEP) (pancreas carcinoma, MIA-PACA-2 and colon adenocarcinoma, HT-29) cell lines were obtained from DSMZ (Germany). HBL and MM162 were cultured in Ham's F10 medium (Lonza), COLO-677 and HT-29 were cultured in RPMI-1640 (Sigma), EJM was cultured in Iscove's MDM (Gibco, Invitrogen, UK) and MIA-PACA-2 was cultured in DMEM (Sigma). All media were supplemented with L-glutamine (Sigma), penicillin (Sigma), streptomycin (Gibco, Invitrogen, UK) and kanamycin (Bio Basic) at standard concentrations as well as with 10% fetal bovine serum, except EJM cell line with 20%. Cells were maintained in their respective growth medium at 37 °C in a humidified 95% air and 5% CO_2 atmosphere. All cell lines were regularly checked for mycoplasma contamination using MycoAlert® Mycoplasma Detection Kit (Lonza, Rockland, ME, USA). Cell lines were chosen based on two characteristics: (1) cell lines derived from malignancies expressing SSTR (melanoma [25,26], multiple myeloma [27–30], pancreatic [31] and colon [32] carcinoma) in order to ensure the presence of the target, which was verified later on and (2) cell lines derived from malignancies exhibiting a range of intrinsic radiosensitivities (from radiosensitive (myeloma) to radioresistant (melanoma), and intermediate radiosensitivity (pancreatic and colorectal cancers), classified as such based on the mean survival at 2 Gy of EBRT [33]), providing us diversified cell populations valuable for the investigation of the influence of biological factors in radiosensitivity.

2.2. Radiopharmaceuticals production

[^{68}Ga]Ga-DOTATATE and [^{177}Lu]Lu-DOTATATE were produced within the radiopharmacy facility of the department of nuclear medicine at Institut Jules Bordet, as previously described [34,35]. In brief, labelling was performed on a synthesis module with disposable cassettes (Modular Pharmlab, Eckert & Ziegler, Germany) using non-carrier added $^{177}LuCl_3$ (EndolucinBeta, ITG, Germany) or $^{68}GaCl_3$ (GalliEo, IRE, Belgium) and DOTATATE (Bachem AG) in sodium ascorbate/acetate buffer at high temperature (80 °C/95 °C). The obtained raw radioactive solution was purified by solid phase extraction on a C18 cartridge and subsequent sterile filtration over a 0.22 μm filter (included in the disposable cassette). All quality controls have been performed according to the European Pharmacopoeia.

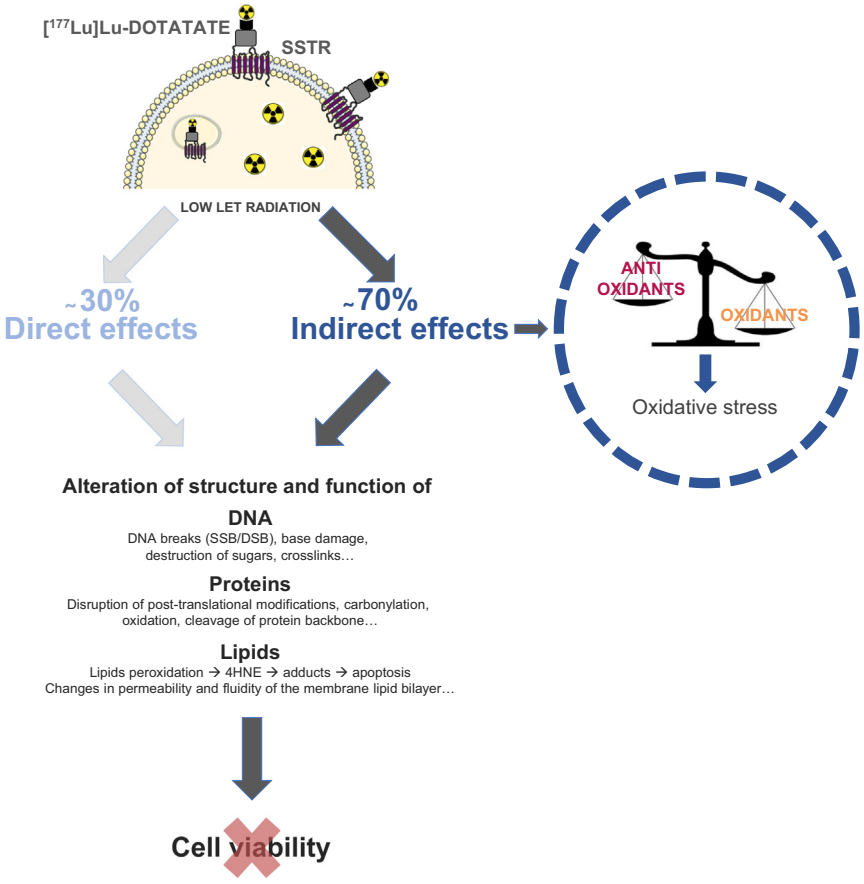

Fig. 1. Radiation biology of [^{177}Lu]Lu-DOTATATE. The therapeutic efficacy of [^{177}Lu]Lu-DOTATATE relies on IR-induced cell damages. In case of irradiation with a low LET emitter such as ^{177}Lu, the majority of the biological effect is due to indirect effects of IR. Indirect effects are mediated by the generation of ROS (oxidants). If oxidant molecules exceed the antioxidant capacity of the cell, oxidative stress occurs, resulting in oxidative damages to DNA, proteins and lipids. SSTR = somatostatin receptor; LET = linear energy transfer; SSB = single strand break; DSB = double strand break; 4HNE = 4-hydoxynonenal.

2.3. [^{177}Lu]Lu-DOTATATE treatment

Cells were seeded in 12-well plates (Corning® CellBIND® Multiple Well Plate, Merck) at different densities (HBL and COLO-677: 1000 cells/well; MM162: 2000 cells/well; EJM: 4000 cells/well; MIA-PACA-2 and HT-29: 200 cells/well). The next day (corresponding to day 0), 5 MBq of [^{177}Lu]Lu-DOTATATE was added in each well, with a minimum of three technical replicates. After 4 h of incubation at 37 °C, the medium containing [^{177}Lu]Lu-DOTATATE was removed and replaced with fresh medium. Three days after treatment, the medium was replaced with fresh medium. Cells were kept in culture until used for cell survival assessment.

2.4. Radiopharmaceuticals uptake assay

Cells were seeded in 24-well plates (HBL, MIA-PACA-2 and HT-29: 3×10^5 cells/well; MM162: 1×10^5 cells/well; COLO-677 and EJM: 5×10^5 cells/well) and the next day adherent cells in monolayer were incubated at 37 °C with the desired radiopharmaceutical in four technical replicates as follows: 2 h with 100 kBq of [^{68}Ga]Ga-DOTATATE/[^{177}Lu]Lu-DOTATATE for the SSTR-based uptake assay and 1 h with 100 kBq of [^{18}F]fluorodeoxyglucose ([^{18}F]FDG, Hôpital Erasme, Brussels, Belgium) in phosphate-buffered saline (PBS) (Lonza) for the glucose metabolism assessment. Cells were subsequently washed twice with ice-cold PBS, lysed with 1 M NaOH and then transferred in tubes to measure the internalized activity. Measurements were performed with a gamma well counter 2480 WIZARD2 (Perkin Elmer) with background and decay correction. Reference activity standards were also quantified in order to normalize the internalized activity with the added activity.

2.5. RT-qPCR

Total RNA was extracted from cell lines using the RNeasy Mini Kit (Qiagen) and RNA concentrations and quality were determined by the NanoDrop® ND-1000 Spectrophotometer. cDNA was synthesized using a standard reverse transcription method (qScriptTM cDNA Super Mix (Quanta Biosciences)). Expression of the following genes was assessed by quantitative PCR using the Power SYBR Green PCR Master Mix (Applied Biosystems): *SSTR2*, *CAT*, *GPX1*, *PARP1*, *XRCC1*, *XRCC4*, *XRCC5*, *XRCC6*, *XRCC7*, *RPA*, *RAD51*, *BRCA2*, *BRCA1*, *ATM* and *18S rRNA*. PCR reactions were performed in four technical replicates and run on QuantStudio 3 Real-Time PCR system (ThermoFisher Scientific) at 95 °C for 10 min followed by 40 cycles at 95 °C for 15 s and 60 °C for 1 min. Relative quantification was determined by normalizing the quantification cycle (Cq) of target genes with the Cq of the reference gene (18S rRNA) using the $2^{-\Delta Cq}$ method. Primers sequences have been chosen from the PrimerBank database. Amplification efficiency was assessed and only primers with efficiency between 90 and 110% have been selected. Primers were obtained from ThermoFisher Scientific. Primers characteristics are described in supplemental material.

2.6. Immunocytochemistry

Cell pellets were washed using PBS, then fixed with formaldehyde for 30 min and embedded in agar. The agar-cell mix was transferred to a syringe's tube, kept on ice and then transferred in a standard tissue-processing cassette. All samples were fixed in formaldehyde, dehydrated and then embedded in paraffin. Immunocytochemistry was carried out on 4 μm paraffin-embedded slides using the SSTR2 antibody (pre-diluted, reference 2-SO088-10, Diagomics) and the iVIEW DAB detection kit on the BenchMark XT system (Ventana). Briefly, conjugation of biotinylated goat-anti-rabbit IgG with streptavidin-HRP allowed the visualization of the brown colored precipitate at the site of specific antibody binding after the addition of HRP substrates (DAB and H_2O_2). Stained slides were scanned using the scanner Nanozoomer NDP (Hamamatsu Photonics). The percentage of SSTR2 positive cells was determined visually.

2.7. Cell survival assay

Cell survival was assessed by crystal violet. The culture medium was removed and cells were gently washed with PBS, fixed with 1% glutaraldehyde (Merck) in PBS for 15 min and stained with 0.1% crystal violet (Sigma) in water for 30 min. The plates were washed under running tap water and subsequently lysed with 0.2% Triton X-100 (Roche) in water for 90 min. The associated absorbance was measured at 590 nm using the BioTek® 800™ TS Absorbance Reader.

2.8. Glutathione quantification

Reduced glutathione (GSH) was assessed using the Quantification kit for oxidized and reduced glutathione (Sigma) according to manufacturer's instructions. In brief, cells were lysed by repeated freeze-thaw cycles. The buffer solution was added to samples (in triplicates) in a 96-well plate. After 1 h incubation at 37 °C, the substrate (5,5′-dithiobis (2-nitrobenzoic acid)) (DTNB), coenzyme and enzyme (GSH reductase) were added in wells, followed by 10 min incubation at 37 °C. Absorbance was read at 405 nm using a microplate reader (Thermo Labsystems Multiskan EX). Total GSH (oxidized and reduced) and oxidized GSH concentration were determined using calibration curves. Reduced GSH concentration was determined by subtracting the amount of oxidized GSH from the total amount of GSH.

2.9. Superoxide dismutase activity measurement

Total superoxide dismutase (SOD) activity was assessed using the HT Superoxide dismutase assay kit (Trevigen) according to the manufacturer's instructions. Briefly, cell pellets were mixed with Cell Extraction Buffer and kept on ice during 30 min, with periodic vortexing. Following centrifugation, the pellet was eliminated and protein concentration was determined in the supernatant. Master Mix was added to cell extracts (in triplicates). Immediately after the addition of xanthine solution, absorbance measurements were done at 450 nm every minute for 10 min. The extent of reduction in the appearance of WST-1 formazan is a measure of SOD activity present in the sample. One unit of SOD reduces the rate of WST-1 formazan formation by 50%.

2.10. ROS measurement

Cells were seeded in Petri dishes (1 million cells/dish). The next day, cells were treated with 100 μM paraquat dichloride (Sigma) for 24 h. All cell lines were non-confluent at the time of experiment to avoid any ROS increase associated with high cell density [36]. The percentage of ROS negative and ROS positive cells was assessed using the Muse® Oxidative Stress Kit (Luminex) according to the manufacturer's instructions. Briefly, cells were harvested and re-suspended in 1× assay buffer. The cells in suspension were then incubated at 37 °C with the Muse® Oxidative Stress working solution for 30 min. Every sample was then thoroughly mixed and run on the Muse® Cell Analyzer (Merck). Kaluza Flow Cytometry Analysis v2.1 software (Beckman Coulter) was used for the analysis. Test principle is based on the fluorescence detection of the oxidized dihydroethidium (DHE) by superoxide anions and allows to distinguish two population of cells: ROS(−) (live cells) and ROS(+) (cells exhibiting ROS).

2.11. Cell proliferation

Cells were seeded in 6-well plates (HBL, MM162, MIA-PACA-2 and HT-29: 25000 cells/well; COLO-677 and EJM: 50000 cells/well). At each time point (day 1, 2, 3, 4 and 7), cells were harvested and mixed with the Muse® Count & Viability Reagent. After 5 min of incubation,

every sample was then thoroughly mixed and run on the Muse® Cell Analyzer (Merck).

2.12. Cell cycle analysis

Cells were seeded in Petri dishes (MM162: 1,5 million cells/dish; HBL, MIA-PACA-2 and HT-29: 2 million cells/dish; COLO-677 and EJM: 4 million cells/dish). The next day, non-confluent cells were harvested, washed once with PBS and fixed in 70% ethanol at −20 °C for 2 h. Cells were then centrifuged for 5 min and washed once with PBS. After another centrifugation step, cells were resuspended in 400 μL of staining solution per million cells (50 μg/mL propidium iodide (ThermoFisher) in PBS) and incubated for 10 min at room temperature. Samples were acquired on a flow cytometer (Navios EX, Beckman Coulter) and results were analyzed using Kaluza Flow Cytometry Analysis v2.1 software (Beckman Coulter).

2.13. Statistical analysis

Statistical analysis was performed using the GraphPad Prism 7 software (GraphPad Software, La Jolla, CA, USA). After normality verification using the Shapiro-Wilk test, parametric *t*-test was performed. Significance is indicated as: $^{*}p \leq 0.05$ - $^{**}p \leq 0.01$ - $^{***}p \leq 0.001$.

3. Results

3.1. SSTR2 expression and functionality

SSTR2 expression was assessed in all cell lines at the genomic and proteomic levels as well as its functionality. At the mRNA level, SSTR2 was expressed in all cell lines, with varying levels of expression. The highest expression levels were observed in the two melanoma cell lines (HBL and MM162), whereas the lowest was observed in the EJM multiple myeloma cell line, being 100 times lower than HBL (Fig. 2A). Immunocytochemistry staining confirmed SSTR2 protein expression in all cell lines, in >50% of cells (HBL: 86%, MM162: 74%, COLO-677: 65%, EJM: 60%, MIA-PACA-2: 71%, HT-29: 58%). Staining intensity varied from strong (HBL) to moderate (MM162, MIA-PACA-2, HT-29) and low (COLO-677, EJM) (Fig. 2B). To confirm SSTR2 functionality, uptake assays using [^{68}Ga]Ga-DOTATATE and [^{177}Lu]Lu-DOTATATE were performed. Uptake of both radiotracers was similar in all cell lines. Melanoma cell lines (HBL and MM162) had the highest uptake, while multiple myeloma cell lines (COLO-677 and EJM) had the lowest one, being about 15 times lower than the melanoma cell lines uptake (Fig. 3). These results were in line with SSTR2 protein expression.

3.2. Proliferation rate

The proliferation rate of the cell lines was assessed as a parameter for radiosensitivity. Cell count over time allowed to determine a cell doubling time that reflects the cell proliferation rate under the intended experiment conditions and timing. The most proliferative cell lines were the GEP ones (MIA-PACA-2 and HT-29) with a doubling time of 27.52 ± 0.03 and 26.28 ± 0.81 h respectively. The lowest proliferative cell lines were EJM (43.32 ± 4.29 h) and MM162 (42.81 ± 1.77 h), and HBL (28.57 ± 0.07 h) and COLO-677 (30.60 ± 0.64 h) were in between (Fig. 4A and B).

3.3. Glucose metabolism

In order to evaluate if metabolism could be associated with [^{177}Lu]Lu-DOTATATE sensitivity, glucose metabolism was quantified in each cell line using [^{18}F]FDG uptake assay. Cell lines had varying glucose metabolism rates, as represented by varying levels of [^{18}F]FDG accumulation in cells. MM162 and HT-29 had the highest glucose metabolism (respectively 0.430 ± 0.018 and 0.449 ± 0.035% of added radioactivity per 10^6 cells) while multiple myeloma cell lines COLO-677 and EJM had the lowest (respectively 0.096 ± 0.001 and 0.033 ± 0.002% of added radioactivity per 10^6 cells). HBL and MIA-PACA-2 had similar and intermediate values (respectively 0.163 ± 0.001 and 0.148 ± 0.025% of added radioactivity per 10^6 cells) (Fig. 5).

3.4. DNA repair genes expression

The basal expression of DNA repair genes was analyzed to evaluate if it could impact the response to [^{177}Lu]Lu-DOTATATE in the six cell lines (Fig. 6). Genes involved in the repair of DNA single- and double-strand

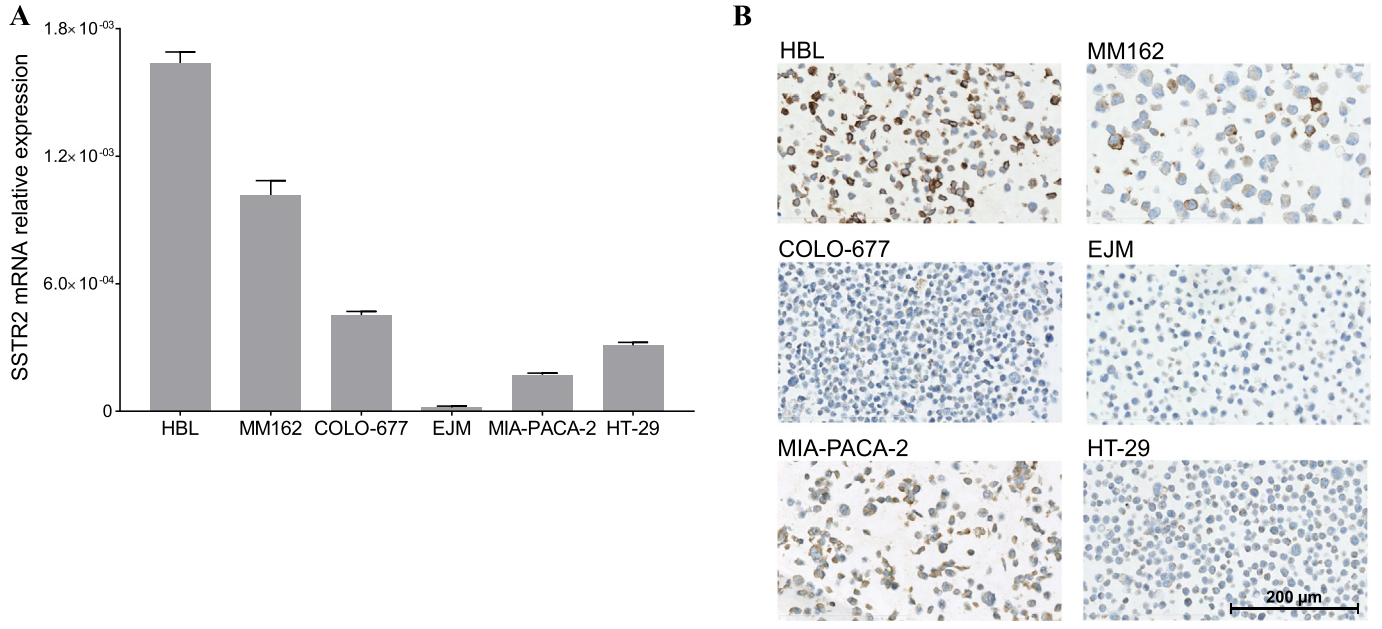

Fig. 2. SSTR2 expression in melanoma (HBL and MM162), multiple myeloma (COLO-677 and EJM) and GEP (MIA-PACA-2 and HT-29) cell lines. (A) mRNA relative expression. Results are represented as mean expression levels ± SEM ($n = 24$ from 6 independant experiments) and are normalized against the reference gene *18S rRNA* that was stable among cell lines. (B) Representative illustration of immunocytochemical staining. Brown staining represents SSTR2. Magnification 40×. (For interpretation of the references to colour in this figure legend, the reader is referred to the web version of this article.)

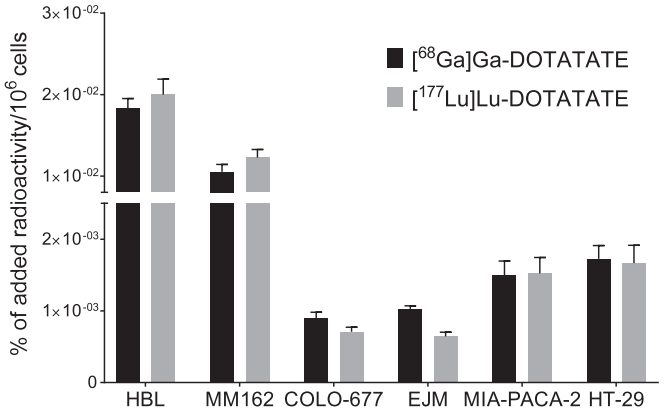

Fig. 3. [^{68}Ga]Ga/[^{177}Lu]Lu-DOTATATE uptake in melanoma (HBL and MM162), multiple myeloma (COLO-677 and EJM) and GEP (MIA-PACA-2 and HT-29) cell lines. Results are represented as mean ± SEM (n = 20 from 5 independant experiments) of the percentage of the added radioactivity, normalized by 10^6 cells.

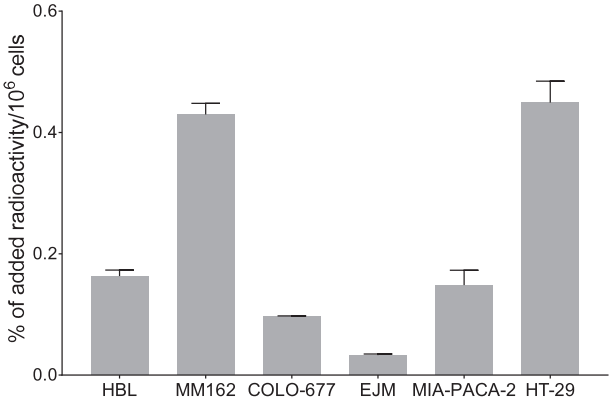

Fig. 5. [^{18}F]FDG uptake in melanoma (HBL and MM162), multiple myeloma (COLO-677 and EJM) and GEP (MIA-PACA-2 and HT-29) cell lines. Results are represented as mean ± SEM (n = 24 from 6 independant experiments) of the percentage of the added radioactivity, normalized by 10^6 cells.

breaks (SSB and DSB), via the base excision repair (BER) and the non-homologous end joining (NHEJ) or homologous recombination (HR) pathways respectively, were selected. PARP1 expression was the highest in COLO-677 (0.448 ± 0.033), followed by EJM (0.135 ± 0.004), MIA-PACA-2 (0.117 ± 0.002) and HT-29 (0.088 ± 0.004). The expression was the lowest and similar in the HBL and MM162 melanoma cell lines, being 0.039 ± 0.002 and 0.041 ± 0.009 respectively (Fig. 6A). XRCC1 expression was more than ten times lower compared to PARP1 expression and ranged from 0.0010 ± 0.0002 (COLO-677 and MM162) to 0.0030 ± 0.0001 (HT-29) (Fig. 6B). Combined expression of genes involved in the repair of DSB was the highest in COLO-677 (0.1774 ± 0.0051 (NHEJ genes) and 0.0334 ± 0.0034 (HR genes)) and the lowest in HBL (0.0433 ± 0.0013 (NHEJ genes) and 0.0103 ± 0.0004 (HR genes)) (Fig. 6C and D).

3.5. Cell cycle phases

Cell cycle influences radiosensitivity, which is the highest during mitosis and the lowest during S phase. Therefore, the percentage of cells in each phase of the cell cycle was assessed, at the moment of exposure to the treatment (Fig. 7). The percentage of cells in the G2/M phase ranged from 11.68 ± 0.97% (MM162) to 33.49 ± 0.52% (MIA-PACA-2), with intermediate values for EJM (15.80 ± 0.92%), HBL (18.07 ± 0.87%), COLO-677 (24.78 ± 2.90%) and HT-29 (27.55 ± 4.42%). The percentage of cells in the S phase was the highest in GEP cell lines (MIA-PACA-2: 15.56 ± 0.41%; HT-29: 13.01 ± 2.56%), followed by multiple myeloma cell lines (COLO-677: 11.20 ± 0.83%; EJM: 10.18 ± 1.09%) and was the lowest in melanoma cell lines (HBL: 9.75 ± 0.38%; MM162: 7.44 ± 1.60%).

3.6. Antioxidant defences

First line antioxidant defences, namely GSH, catalase, GSH peroxidase and SOD, were assessed in all cell lines to evaluate their relationship with [^{177}Lu]Lu-DOTATATE sensitivity (Fig. 8). Baseline reduced GSH levels varied among cell lines, with the lowest observed in the multiple myeloma cell lines (COLO-677: 35.6 ± 1.3 μmol/L/10^6cells; EJM 30.5 ± 2.5 μmol/L/10^6cells) and the highest observed in the MM162 melanoma (203.4 ± 3.2 μmol/L/10^6cells) and the MIA-PACA-2 pancreatic (142.4 ± 5.1 μmol/L/10^6cells) cell lines. HBL and HT-29 had intermediate value of 95.4 ± 8.5 and 94.6 ± 2.7 μmol/L/10^6cells respectively (Fig. 8A). Combined catalase and GSH peroxidase expression was significantly ($p < 0.05$) higher in HT-29 compared to all the other cell lines (Fig. 8B). SOD activity was the highest in COLO-677 (124.1 ± 2.4 U/mg protein) and MIA-PACA-2 (119.0 ± 8.6 U/mg protein), and the lowest in HT-29 (48.1 ± 2.3 U/mg protein) (Fig. 8C). To further evaluate antioxidant defences and more precisely the capacity of cell lines to detoxify ROS, the percentage of ROS positive and negative cells was assessed following treatment with the ROS inducer paraquat. The baseline levels of ROS positive cells were about twice higher in MM162 (27.4%), MIA-PACA-2 (22.4%) and HT-29 (27.9%) cell lines com-

A

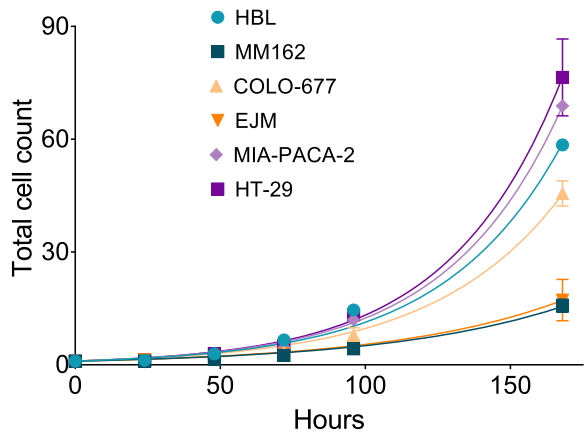

B

Cell line	Doubling time (hours)
HBL	28.57 ± 0.07
MM162	42.81 ± 1.77
COLO-677	30.60 ± 0.64
EJM	43.32 ± 4.29
MIA-PACA-2	27.52 ± 0.03
HT-29	26.28 ± 0.81

Fig. 4. Proliferation rate of melanoma (HBL and MM162), multiple myeloma (COLO-677 and EJM) and GEP (MIA-PACA-2 and HT-29) cell lines. (A) Total cell count over time, normalized to number of cells plated on day 0, representing mean ± SEM (n = 3 from 3 independant experiments). (B) Cell lines doubling time calculated from growth curves (mean ± SEM).

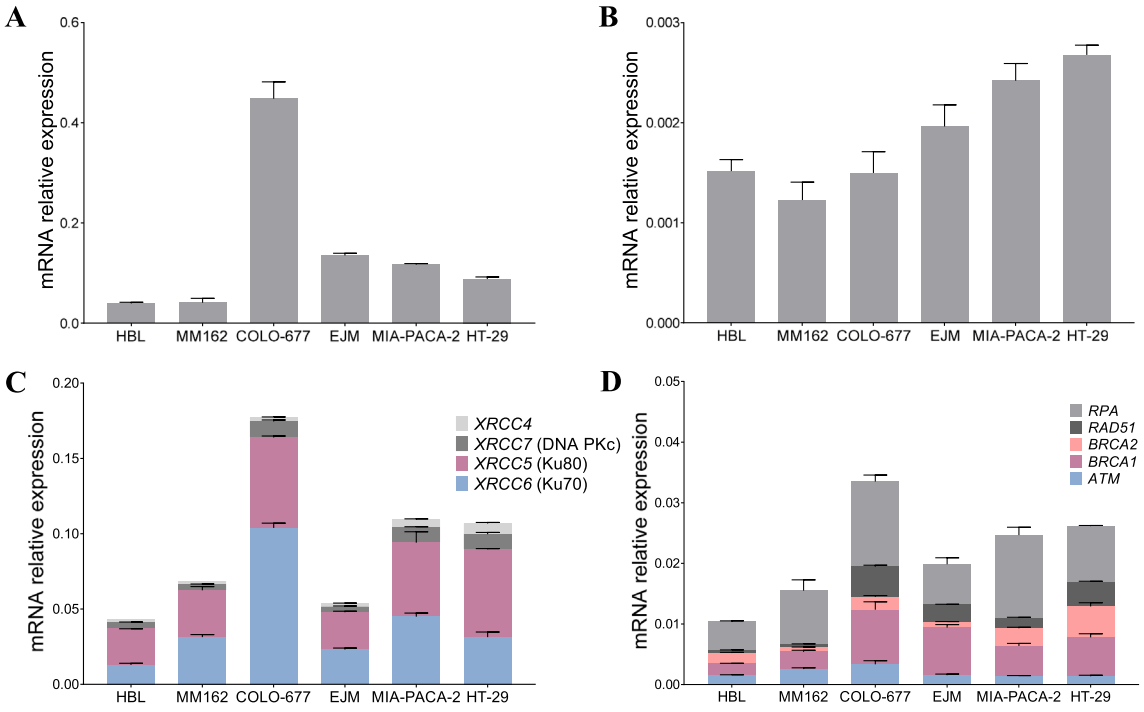

Fig. 6. mRNA expression of DNA damage repair genes in melanoma (HBL and MM162), multiple myeloma (COLO-677 and EJM) and GEP (MIA-PACA-2 and HT-29) cell lines. Base excision repair genes expression (A) *PARP1* and (B) *XRCC1*. (C) Non-homologous end joining genes expression (D) Homologous recombination genes expression. Results are represented as mean expression levels ± SEM ($n = 12$ from 3 independant experiments) and normalized against the reference gene *18S rRNA* that was stable among cell lines.

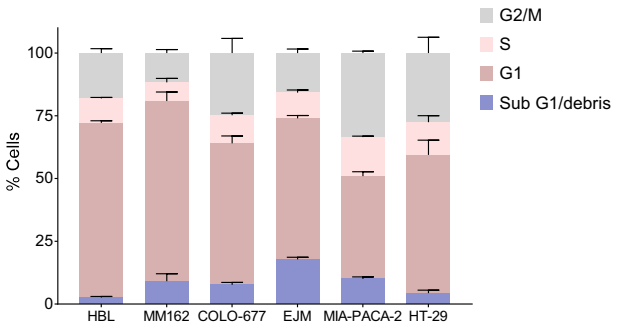

Fig. 7. Cell cycle distribution in melanoma (HBL and MM162), multiple myeloma (COLO-677 and EJM) and GEP (MIA-PACA-2 and HT-29) cell lines. Results are represented as mean ± SEM (n = 3 from 3 independant experiments).

pared to HBL (8.2%), COLO-677 (13.5%) and EJM (9.7%) (Fig. 9A). The percentage of ROS positive cells after paraquat treatment was significantly increased and the highest in both multiple myeloma cell lines COLO-677 (+ 59.8 ± 17.9%, $p = 0.03$) and EJM (+ 54.9 ± 10.9%, $p = 0.01$) followed by the HBL cell line (+ 31.7 ± 8.3%, $p = 0.02$). In the three other cell lines the percentage of ROS positive cells remained unchanged (MM162: - 4.9 ± 2.4%, $p = 0.07$; HT-29: - 5.9 ± 15.2%, $p = 0.7$) or was non significantly elevated (MIA-PACA-2: + 21.6 ± 10.7%, $p = 0.09$) (Fig. 9A and B).

3.7. Cell survival after [^{177}Lu]Lu-DOTATATE treatment

In order to assess the radiosensitivity of the different cell lines to IR from [^{177}Lu]Lu-DOTATATE, cell survival was evaluated (Fig. 10). [^{177}Lu]Lu-DOTATATE induced a time-dependent decrease of cell survival in all cell lines, except in the colon HT-29 whose survival was not affected by the treatment (Fig. 10A). At day 10, significant (all p values <0.001) reduction of cell survival was observed in HBL (−26% ± 4%), MM162 (−13% ± 3%), COLO-677 (−33% ± 2%), EJM (−22% ± 2%) and MIA-PACA-2 (−14% ± 3%) (Fig. 10A and B). Based on these results,

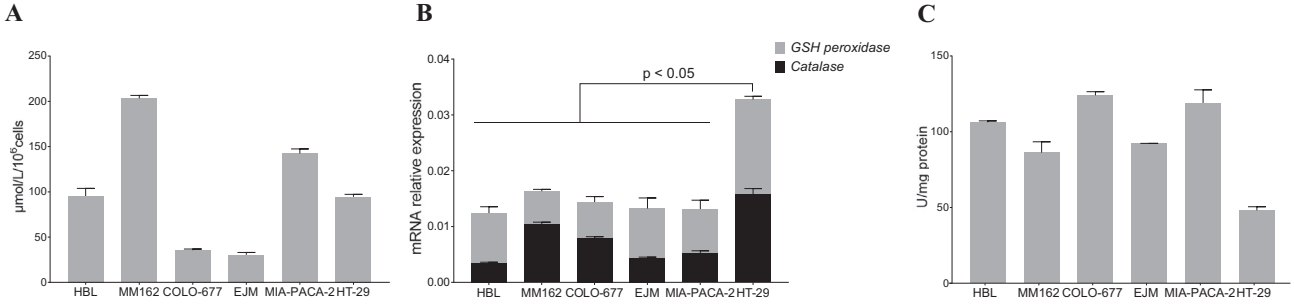

Fig. 8. Expression and activity of main antioxidant defences in melanoma (HBL and MM162), multiple myeloma (COLO-677 and EJM) and GEP (MIA-PACA-2 and HT-29) cell lines. (A) GSH levels. Results are represented as mean ± SEM ($n = 9$ from 3 independant experiments) and normalized by 10^6 cells. (B) *Catalase* and *GSH peroxidase* mRNA relative expression. Results are represented as mean expression levels ± SEM (n = 12 from 3 independant experiments) and normalized against the reference gene *18S rRNA* that was stable among cell lines. (C) Total SOD (SOD1 and SOD2) enzymatic activity. Results are represented as mean ± SEM ($n = 6$ from 2 independant experiments).

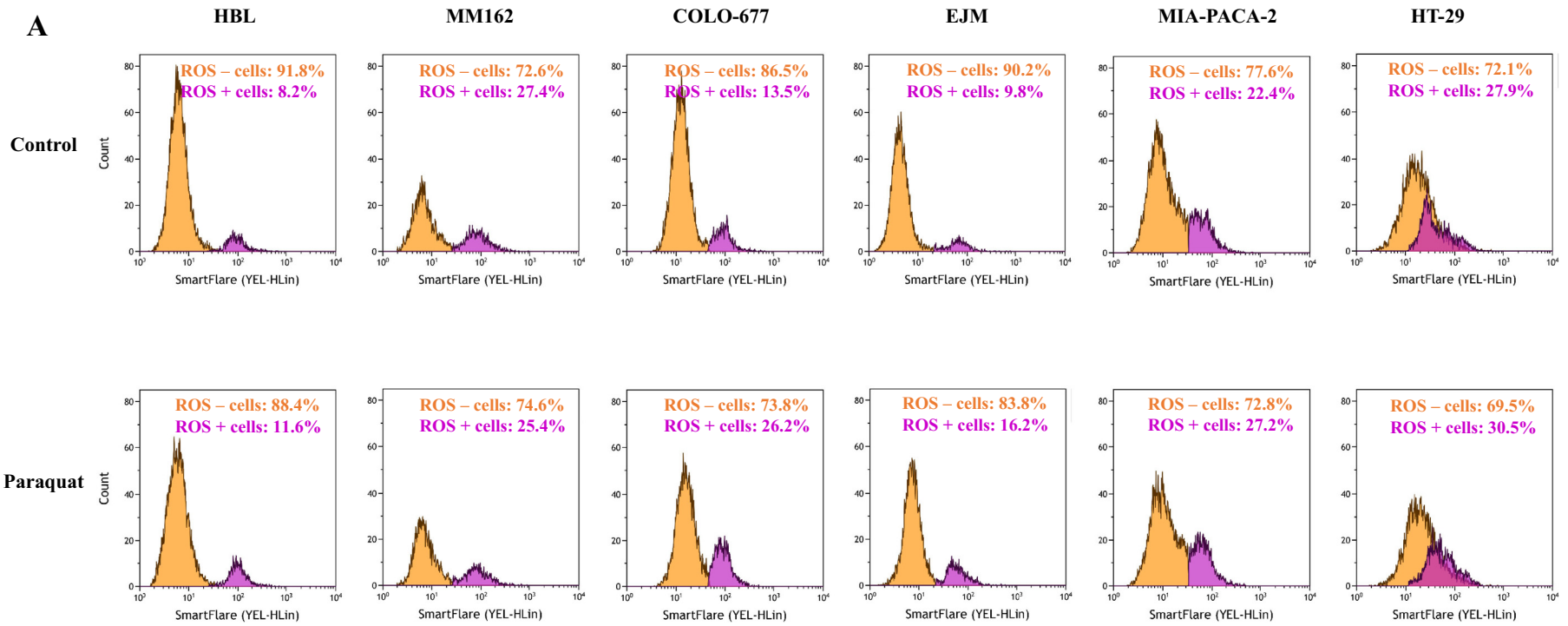

Fig. 9. ROS negative/positive cell percentage in melanoma (HBL and MM162), multiple myeloma (COLO-677 and EJM) and GEP (MIA-PACA-2 and HT-29) cell lines after stimulation with 100 μM paraquat for 24 h. (A) Representative flow cytometry graph of the percentage of ROS negative (orange) and ROS positive (purple) cells in control and treated (paraquat) conditions. (B) Percentage of ROS positive cells in treated (paraquat) samples, normalized to the percentage of ROS positive cells in non-treated counterparts. Results are represented as mean ± SEM (n = 3 from 3 independant experiments). Dotted line represents ROS positive cells in the non-treated condition. * $p \leq 0.05$ and ** $p \leq 0.01$. (For interpretation of the references to colour in this figure legend, the reader is referred to the web version of this article.)

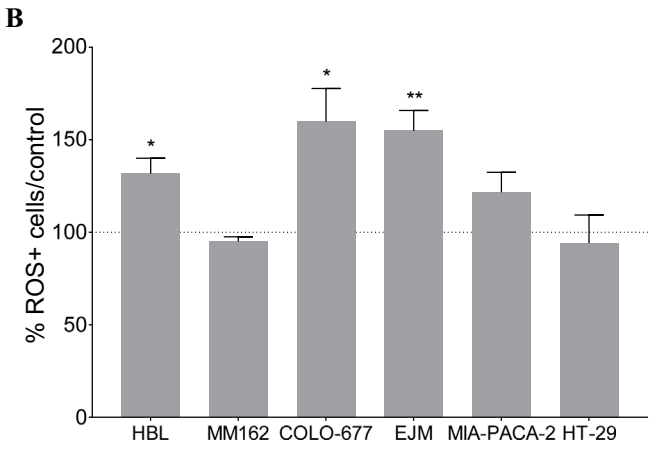

Fig. 9 (*contiuned*).

multiple myeloma (COLO-677 and EJM) as well as the HBL melanoma cell lines were considered as the most sensitive cell lines, while the MM162 and the GEP cell lines (MIA-PACA-2 and HT-29) had an intermediate to low sensitivity to [^{177}Lu]Lu-DOTATATE (Table 1).

3.8. Relationship between biological factors and sensitivity to [^{177}Lu]Lu-DOTATATE

Basal characteristics of the different cell lines were confronted to the cell survival results to evaluate if they were associated with [^{177}Lu]Lu-DOTATATE sensitivity (Fig. 11). A 20% threshold was chosen as the best cut off that could separate the six cell lines into two equivalent groups (round number median). Using this cut off, the six cell lines were separated into two groups of sensitivity to [^{177}Lu]Lu-DOTATATE: COLO-677, HBL and EJM with a decrease in cell survival of >20%, and MIA-PACA-2, MM162 and HT-29 with a decrease in cell survival of <20%. The total antioxidant capacity, evaluated by the percentage of ROS production after treatment with the ROS inducer paraquat, GSH levels and glucose metabolism were significantly lower ($p < 0.05$) in the group with a higher sensitivity compared to the group with a lower sensitivity to [^{177}Lu]Lu-DOTATATE. SSTR ($p = 0.64$), proliferation rate ($p = 0.74$), cell cycle ($p = 0.55$), DNA repair (BER $p = 0.22$; NHEJ $p = 0.93$; HR $p = 0.91$), combined catalase and GSH peroxidase expression ($p = 0.42$) and SOD activity ($p = 0.41$) were not significantly different between the two groups (Fig. 11B).

Table 1
Classification of cell lines into two different groups of sensitivity to [^{177}Lu]Lu-DOTATATE based on the cell survival at day 10.

Sensitivity to [^{177}Lu]Lu-DOTATATE	
High	Intermediate/low
HBL (−26 ± 4%)	MM162 (−13 ± 3%)
COLO-677 (−33 ± 2%)	MIA-PACA-2 (−14 ± 3%)
EJM (−22 ± 2%)	HT-29 (−1 ± 2%)

4. Discussion

The aim of our study was to evaluate the relationship between SSTR expression/functionality as well as several key parameters of intrinsic

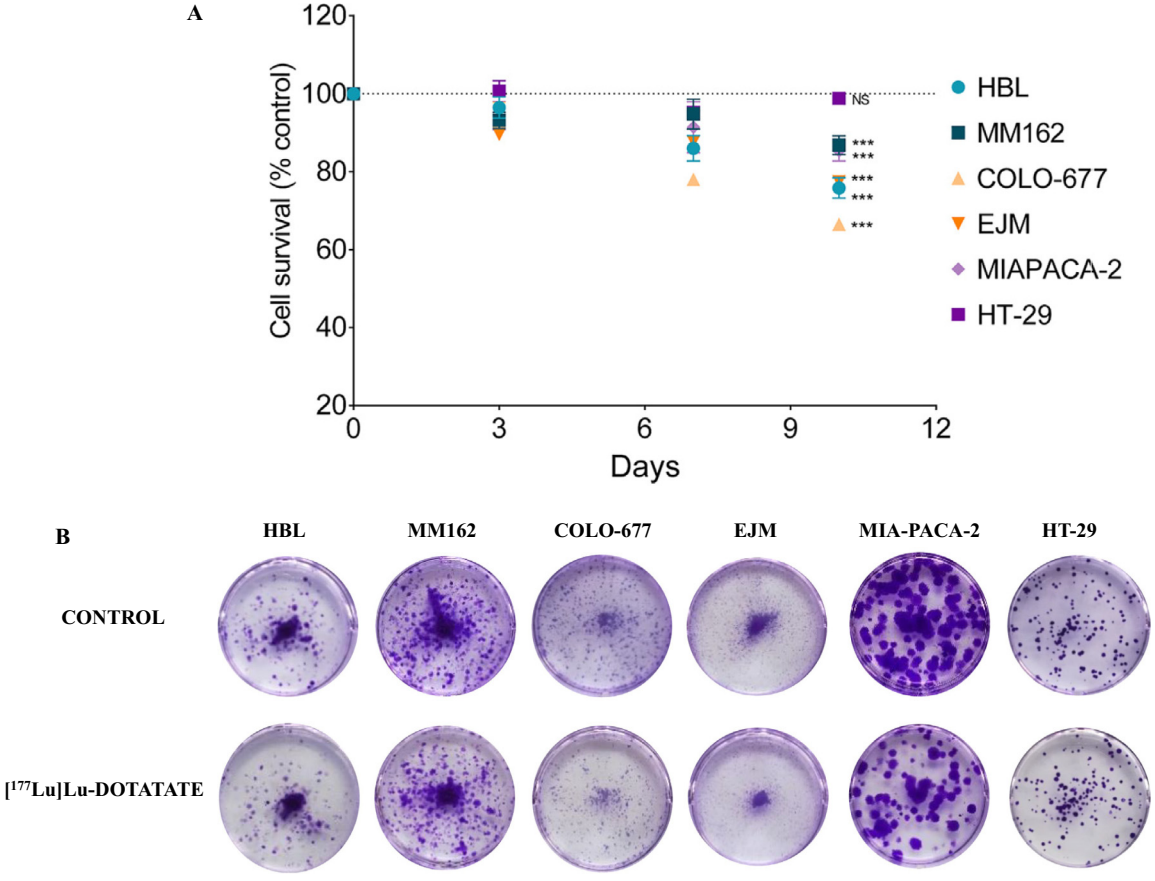

Fig. 10. Effect of [^{177}Lu]Lu-DOTATATE on survival of melanoma (HBL and MM162), multiple myeloma (COLO-677 and EJM) and GEP (MIA-PACA-2 and HT-29) cell lines. (A) Cell survival was assessed 3, 7 and 10 days after 4 h incubation with 5 MBq of [^{177}Lu]Lu-DOTATATE. Results are expressed as a percentage of the non-treated control and are represented as mean ± SEM (n = 20 from 5 independant experiments). Black dotted line represents 100% survival. *** $p \leq 0.001$. (B) Representative crystal violet staining 10 days after 4 h incubation with 5 MBq of [^{177}Lu]Lu-DOTATATE. (For interpretation of the references to colour in this figure legend, the reader is referred to the web version of this article.)

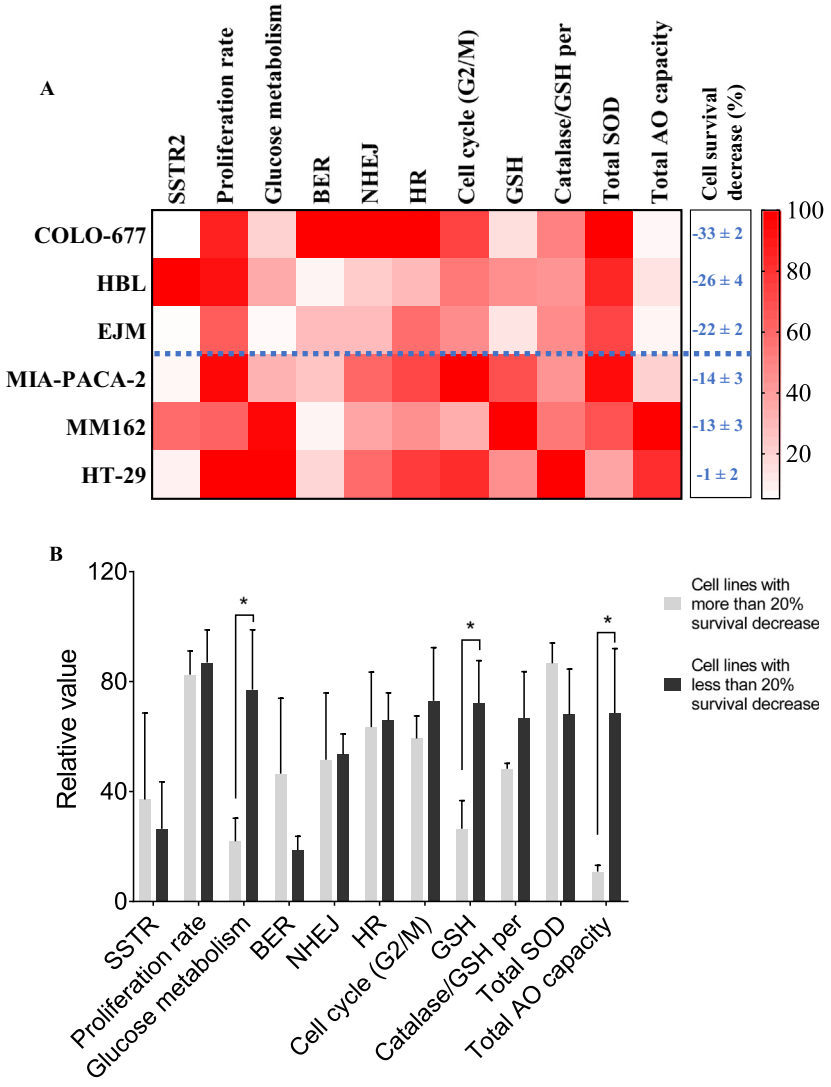

Fig. 11. Basal characterization of SSTR2 and intrinsic radiosensitivity characteristics as well as survival after [^{177}Lu]Lu-DOTATATE in melanoma (HBL and MM162), multiple myeloma (COLO-677 and EJM) and GEP (MIA-PACA-2 and HT-29) cell lines. (A) Heat-map and (B) graphical representation of the normalized characteristics in the different cell lines. SSTR2 ([^{68}Ga]Ga-DOTATATE), proliferation rate (inversed doubling time), glucose metabolism, DNA repair genes (BER, NHEJ and HR), cell cycle (G2/M phase), antioxidant defences (GSH, catalase/GSH peroxidase, SOD) and the total antioxidant (AO) capacity (inversed ROS induction). The results for each characteristics have been normalized to the highest obtained value of each cell line, expressed as 100. Cell lines were separated based on a cut-off value of 20% decrease in cell survival after treatment with [^{177}Lu]Lu-DOTATATE (blue dotted line). (B) Results are expressed as mean of the 3 cell lines ± SEM. * $p \leq 0.05$. (For interpretation of the references to colour in this figure legend, the reader is referred to the web version of this article.)

radiosensitivity (i.e. proliferation rate, glucose metabolism, DNA repair, cell cycle and antioxidant defences) and sensitivity to IR from [^{177}Lu]Lu-DOTATATE in a panel of cancer cell lines. Among all the parameters assessed under basal condition (i.e. without any treatment), the total antioxidant capacity of cells, the GSH levels and the glucose metabolism were significantly lower in cell lines whose survival was reduced by >20% following treatment with [^{177}Lu]Lu-DOTATATE compared to cell lines whose survival was reduced by <20%. SSTR expression, proliferation rate, DNA repair, cell cycle phase and other antioxidant defences evaluated separately (i.e. SOD, catalase and GSH peroxidase) were not significantly different between the two groups of cell lines (Fig. 11).

SSTR positive disease, visualized by [^{68}Ga]Ga-DOTA-peptides PET/CT [37], is a prerequisite for PRRT. The hypothesis that higher receptor density will lead to greater binding and internalization of the radiolabeled analogue in tumour cells and thus result in greater IR-induced cell damages with PRRT has been investigated by several groups. In our study, SSTR2 functionality, assessed by uptake of [^{68}Ga]Ga- and [^{177}Lu]Lu-DOTATATE, was well reflective of SSTR2 protein expression but could not predict sensitivity to [^{177}Lu]Lu-DOTATATE in our panel of cancer cell lines. Our results are in line with other pre-clinical studies showing that cell lines and even xenograft tumours with the highest SSTR expression levels are not the most sensitive to PRRT [38,39]. On the other hand, in the more complex clinical setting, the assessment of the predictive value of [^{68}Ga]Ga-DOTA-peptides PET/CT [40–44] for response to PRRT generated diverging conclusions. These data suggest that a certain uptake threshold has to be surpassed to consider a therapeutic dose-effect, however the level of SSTR expression cannot solely determine the response to PRRT [45]. Furthermore, the same assumption was raised in the case of another ^{177}Lu-based therapy, namely [^{177}Lu]Lu-PSMA [46]. The response to PRRT with [^{177}Lu]Lu-DOTATATE further depends on intrinsic cellular features [47].

ROS generation and subsequent oxidative damages represent the dominant process associated with low LET radiation such as ^{177}Lu. Therefore the antioxidant capacity of cells might impact their sensitivity to [^{177}Lu]Lu-DOTATATE. In our study, antioxidant defences (SOD, catalase and GSH peroxidase) evaluated separately could not predict [^{177}Lu]Lu-DOTATATE sensitivity. The explanation may reside in the fact that they catalyze only a group of specific reactions [48] while

oxidative reactions occur extremely rapidly, generating a multitude of reactive species requiring different defence mechanisms for their detoxification. In that respect, the highly abundant GSH, acting as a wide range oxidant scavenger and as a co-factor of several enzymes such as GSH peroxidase [49], was significantly lower in the group of cell lines with a higher sensitivity to [^{177}Lu]Lu-DOTATATE compared to the group with a lower sensitivity. Accordingly, this was further supported by the assessment of the antioxidant capacity of cells able to scavenge ROS induced by paraquat in our experiment, which was significantly lower in the group of cells with >20% survival decrease after [^{177}Lu]Lu-DOTATATE treatment compared to the group of cells with <20% survival decrease.

It has been reported that cancer cells display elevated basal ROS levels due, notably, to increased metabolism in comparison with normal cells [50]. They therefore express higher levels of antioxidants to adapt to this oxidative status. Basal ROS levels could therefore be informative about the cells antioxidant capacity. This was observed in our study where the three less sensitive cell lines had the highest ROS basal levels, being about two folds higher than the three more sensitive cell lines.

Glucose metabolism have been implicated in cancer radioresistance [51] and can be evaluated by [^{18}F]FDG uptake assays. In our study, glucose metabolism was significantly lower in the group of cell lines whose survival was reduced by >20% following treatment with [^{177}Lu]Lu-DOTATATE compared to the group of cell lines whose survival was reduced by <20%, in line with the literature. Increased glucose metabolism, while providing a growth advantage, also confers a resistance phenotype to IR. Indeed, the glucose transporter GLUT1 is frequently upregulated in radioresistant tumour cells [51]. Glucose, as well as [^{18}F]FDG, accumulation in cells is mediated by GLUT1 transport through the cell membrane and subsequent phosphorylation by hexokinase in the cytoplasm, generating glucose-6-phosphate. The latter is a common intermediate for glycolysis as well as the pentose phosphate pathway which generates NADPH by the reduction of NADP+ via the action of glucose-6-phosphate dehydrogenase and 6-phosphoglyconate dehydrogenase. NADPH is a reducing equivalent required for antioxidant enzymes function, such as glutathione reductase. Therefore, maintenance of cell redox potential is facilitated by high glycolysis [52,53]. Interestingly, correlation between glucose metabolism and oxidative stress was described, where GLUT1 inhibition enhanced ROS production [54]. Given the role of oxidative stress in IR, this concept is very relevant in our study.

Regarding proliferation rate, it is known that cells with a greater reproductive activity exhibit faster harmful IR-induced effects [9,10]. However, this was not the case for [^{177}Lu]Lu-DOTATATE-treated cells in this study, where the most proliferative cell lines, the GEP ones (MIA-PACA-2 and HT-29), were not the most sensitive to [^{177}Lu]Lu-DOTATATE with HT-29 even being resistant to [^{177}Lu]Lu-DOTATATE. Similarly, in two xenografts tumour models with equivalent [^{68}Ga]Ga-DOTATATE avidity, the more proliferating tumour model AR42J, was less sensitive to [^{177}Lu]Lu-DOTATATE than the D341 [39]. Taken together, our results are in line with the literature showing that the proliferation rate seems not to be determinant in predicting sensitivity to [^{177}Lu]Lu-DOTATATE compared to EBRT.

Radiosensitivity using EBRT was also reported to be variable according to the cell cycle phases and is maximal during the G2/M phase [8]. For each cell line, the proportion of cells in the different cell cycle phases was assessed in our study at the moment of exposure to the treatment. As expected, the proportion of cells in the G2/M phase was reflective of the cell proliferation rate. However, sensitivity to [^{177}Lu]Lu-DOTATATE was independent of the percentage of cells in the radiosensitive G2/M phase in which cells lay before treatment with [^{177}Lu]Lu-DOTATATE. This can be explained by the fact that [^{177}Lu]Lu-DOTATATE treatment is characterized by a continuous and protracted exposure of cells to IR from ^{177}Lu. Therefore, several cell-division cycles will occur while cells were exposed to ^{177}Lu over days, as opposed to EBRT, where the number of cells in each phase of the cell cycle at the time of the irradiation may be more relevant given the short irradiation period (minutes). However, we cannot totally exclude the possibility that the relative distribution of cells within cell cycle phases may contribute to [^{177}Lu]Lu-DOTATATE sensitivity, as is the case for EBRT. Indeed, radiosensitivity in the G2/M phase was attributed to several factors such as insufficient time to repair DNA damage before dividing, inactivation of DNA DSB repair mechanisms [55] as well as DNA condensation.

Differential efficiencies in DNA repair may lead to variable responses to IR [6], including [^{177}Lu]Lu-DOTATATE since it induces DNA damages [38,56,57]. In our study, expression of DNA repair genes could not predict sensitivity to [^{177}Lu]Lu-DOTATATE. This result informs us that, in contrast to Bishay et al. who were able to correlate *RAD51* gene expression with human lymphocytes radiosensitivity to gamma rays [58], this analysis does not provide any predictive value regarding [^{177}Lu]Lu-DOTATATE sensitivity in our six cell lines. Methods that would allow the evaluation of DNA repair capacity, at a functional level, might be more informative. Currently the evaluation of the sensitivity to other DNA damaging agents [59,60] or the evaluation of γH2AX foci after therapy are used as surrogates [61,62]. However, they do not provide predictive information. Sequencing of DNA repair-related genes could also be considered. The lack of functional analysis is a limitation in our study.

Other limitations include the fact that we have investigated a non-exhaustive list of six factors, which are obviously more than six. For instance, the P53 status of cells has not been addressed here. Furthermore, for a thorough evaluation of the contribution of all factors, more cell lines would have been required, using also more in-depth analyses. Investigating all the parameters under [^{177}Lu]Lu-DOTATATE might also bring additional information.

The hereabove mentioned list of intrinsic factors are based on the extensive radiobiology of EBRT. However, given that [^{177}Lu]Lu-DOTATATE works on the basis of intravenous injection of a vector, bringing radiation inside of the tumour, one should be cautious when extrapolating EBRT radiobiology to PRRT. The fact that sensitivity to EBRT does not correlate linearly with the sensitivity to ^{177}Lu further emphasizes differences in these two radiation-based modalities [38]. While DNA damage related factors have always been considered the key determinants for EBRT, our results suggest that antioxidant defences may be major determinants for PRRT sensitivity in vitro. In vivo, however, the parameters assessed might differ and the influence of other parameters on biological effects of [^{177}Lu]Lu-DOTATATE such as the microenvironment, including immune infiltrates [63] and hypoxia that plays a key role in case of low LET radiation, have to be taken into account.

Although recent advances have been made [64,65], there is still a need to investigate tumour biology to understand which biological factors might correlate with a good response to [^{177}Lu]Lu-DOTATATE in particular, but with ^{177}Lu in general [66]. ^{177}Lu has become a popular radioisotope due to its numerous advantages and is now also being use for the therapy of prostate cancers ([^{177}Lu]Lu-PSMA) with promising results. Our findings are therefore relevant beyond NET therapy with PRRT and warrant the investigation of antioxidant defences as a potential factor influencing ^{177}Lu radiosensitivity. To our knowledge, no study as yet evaluated the role of ROS and antioxidant defences with regards to ^{177}Lu-based radionuclide therapy.

In conclusion, our results suggest that antioxidant defences are major determinants in PRRT sensitivity, acting upfront of DNA damage repair mechanisms, and might be considered as a radiosensitivity biomarker for [^{177}Lu]Lu-DOTATATE. Furthermore, they pave the way to new combination treatment strategies that include targeting the antioxidant system where the therapeutic effects of [^{177}Lu]Lu-DOTATATE might be potentiated.

Supplementary data to this article can be found online at https://doi.org/10.1016/j.nucmedbio.2021.03.006.

Acknowledgements and funding

We express our gratitude to “Les Amis de Bordet” for the grant obtained to conduct this study. We thank Hugues Duvillier from the flow

cytometry and cell sorting unit for his assistance in the flow cytometry experiments.

Declaration of competing interest

The authors declare that they have no conflicts of interest.

References

[1] Bushnell DL, Bodeker KL. Overview and current status of peptide receptor radionuclide therapy. Surg Oncol Clin N Am. 2020;29:317–26. https://doi.org/10.1016/j.soc.2019.11.005.

[2] Reubi JC, Schär JC, Waser B, Wenger S, Heppeler A, Schmitt JS, et al. Affinity profiles for human somatostatin receptor subtypes SST1-SST5 of somatostatin radiotracers selected for scintigraphic and radiotherapeutic use. Eur J Nucl Med. 2000;27:273–82.

[3] Strosberg J, El-Haddad G, Wolin E, Hendifar A, Yao J, Chasen B, et al. Phase 3 trial of 177Lu-dotatate for midgut neuroendocrine tumors. N Engl J Med. 2017;376:125–35. https://doi.org/10.1056/NEJMoa1607427.

[4] Brabander T, van der Zwan WA, Teunissen JJM, Kam BLR, Feelders RA, de Herder WW, et al. Long-term efficacy, survival, and safety of [177Lu-DOTA0,Tyr3]octreotate in patients with gastroenteropancreatic and bronchial neuroendocrine tumors. Clin Cancer Res Off J Am Assoc Cancer Res. 2017;23:4617–24. https://doi.org/10.1158/1078-0432.CCR-16-2743.

[5] Kwekkeboom DJ, de Herder WW, Kam BL, van Eijck CH, van Essen M, Kooij PP, et al. Treatment with the radiolabeled somatostatin analog [177Lu-DOTA0,Tyr3] Octreotate: toxicity, efficacy, and survival. J Clin Oncol. 2016. https://doi.org/10.1200/JCO.2007.15.2553.

[6] Goldstein M, Kastan MB. The DNA damage response: implications for tumor responses to radiation and chemotherapy. Annu Rev Med. 2015;66:129–43. https://doi.org/10.1146/annurev-med-081313-121208.

[7] Baert A, Palermo MF, Van Heetvelde M, Verstraete B, Depuydt J, Vierstraete J, et al. Decreased DNA double-strand break repair and enhanced chromosomal radiosensitivity in irradiated non-tumorigenic human breast epithelial cells with a partial BRCA1 or BRCA2 knockdown. World Acad Sci J. 2020;2:19–27. https://doi.org/10.3892/wasj.2020.35.

[8] Pawlik TM, Keyomarsi K. Role of cell cycle in mediating sensitivity to radiotherapy. Int J Radiat Oncol Biol Phys. 2004;59:928–42. https://doi.org/10.1016/j.ijrobp.2004.03.005.

[9] Bergonié J, Tribondeau L. Interpretation of some results of radiotherapy and an attempt at determining a logical technique of treatment/De Quelques Resultats de la Radiotherapie et Essai de fixation d'une technique Rationnelle. Radiat Res. 1959;11:587–8. https://doi.org/10.2307/3570812.

[10] Vogin G, Foray N. The law of Bergonié and Tribondeau: a nice formula for a first approximation. Int J Radiat Biol. 2013;89:2–8. https://doi.org/10.3109/09553002.2012.717732.

[11] Jiang H, Wang H, De Ridder M. Targeting antioxidant enzymes as a radiosensitizing strategy. Cancer Lett. 2018;438:154–64. https://doi.org/10.1016/j.canlet.2018.09.004.

[12] Woolston CM, Al-Attar A, Storr SJ, Ellis IO, Morgan DAL, Martin SG. Redox protein expression predicts radiotherapeutic response in early-stage invasive breast cancer patients. Int J Radiat Oncol Biol Phys. 2011;79:1532–40. https://doi.org/10.1016/j.ijrobp.2010.11.002.

[13] Tulard A, Hoffschir F, de Boisferon FH, Luccioni C, Bravard A. Persistent oxidative stress after ionizing radiation is involved in inherited radiosensitivity. Free Radic Biol Med. 2003;35:68–77. https://doi.org/10.1016/S0891-5849(03)00243-0.

[14] Fisher CJ, Goswami PC. Mitochondria-targeted antioxidant enzyme activity regulates radioresistance in human pancreatic cancer cells. Cancer Biol Ther. 2008;7:1271–9.

[15] Pouget J-P, Lozza C, Deshayes E, Boudousq V, Navarro-Teulon I. Introduction to radiobiology of targeted radionuclide therapy. Front Med. 2015;2. https://doi.org/10.3389/fmed.2015.00012.

[16] Hall EJ, Giaccia AJ. Radiobiology for the radiologist. Lippincott Williams & Wilkins; 2006.

[17] Ogawa Y. Paradigm shift in radiation biology/radiation oncology—exploitation of the "H_2O_2 effect" for radiotherapy using low-LET (linear energy transfer) radiation such as X-rays and high-energy electrons. Cancers. 2016;8. https://doi.org/10.3390/cancers8030028.

[18] Holley AK, Miao L, St. Clair DK, St. Clair WH. Redox-modulated phenomena and radiation therapy: the central role of superoxide dismutases. Antioxid Redox Signal. 2014;20:1567–89. https://doi.org/10.1089/ars.2012.5000.

[19] Ryter SW, Kim HP, Hoetzel A, Park JW, Nakahira K, Wang X, et al. Mechanisms of cell death in oxidative stress. Antioxid Redox Signal. 2006;9:49–89. https://doi.org/10.1089/ars.2007.9.49.

[20] Eves P, Layton C, Hedley S, Dawson RA, Wagner M, Morandini R, et al. Characterization of an in vitro model of human melanoma invasion based on reconstructed human skin. Br J Dermatol. 2000;142:210–22. https://doi.org/10.1046/j.1365-2133.2000.03287.x.

[21] Gembarska A, Luciani F, Fedele C, Russell EA, Dewaele M, Villar S, et al. MDM4 is a key therapeutic target in cutaneous melanoma. Nat Med. 2012;18:1239–47. https://doi.org/10.1038/nm.2863.

[22] Zimmerer RM, Korn P, Demougin P, Kampmann A, Kokemüller H, Eckardt AM, et al. Functional features of cancer stem cells in melanoma cell lines. Cancer Cell Int. 2013;13:78. https://doi.org/10.1186/1475-2867-13-78.

[23] Krayem M, Journe F, Wiedig M, Morandini R, Sales F, Awada A, et al. Prominent role of cyclic adenosine monophosphate signalling pathway in the sensitivity of WTBRAF/WTNRAS melanoma cells to vemurafenib. Eur J Cancer. 2014;50:1310–20. https://doi.org/10.1016/j.ejca.2014.01.021.

[24] Rambow F, Rogiers A, Marin-Bejar O, Aibar S, Femel J, Dewaele M, et al. Toward minimal residual disease-directed therapy in melanoma. Cell. 2018;174:843–855.e19. https://doi.org/10.1016/j.cell.2018.06.025.

[25] Lum SS, Fletcher WS, O'Dorisio MS, Nance RW, Pommier RF, Caprara M. Distribution and functional significance of somatostatin receptors in malignant melanoma. World J Surg. 2001;25:407–12. https://doi.org/10.1007/s002680020102.

[26] Martinez-Alonso M, Llecha N, Mayorga ME, Sorolla A, Dolcet X, Sanmartin V, et al. Expression of somatostatin receptors in human melanoma cell lines: effect of two different somatostatin analogues, octreotide and SOM230, on cell proliferation. J Int Med Res. 2009;37:1813–22. https://doi.org/10.1177/147323000903700617.

[27] Sharma P, Dhull VS, SKC Suman, Bal C, Malhotra A, Kumar R. 68Ga-DOTANOC somatostatin receptor PET-CT imaging in multiple myeloma. Clin Nucl Med. 2014;39:374–5. https://doi.org/10.1097/RLU.0b013e31828e9722.

[28] Sonmezoglu K, Vatankulu B, Elverdi T, Akyel R, Erkan ME, Halac M, et al. The role of 68Ga-DOTA-TATE PET/CT scanning in the evaluation of patients with multiple myeloma: preliminary results. Nucl Med Commun. 2017;38:76–83. https://doi.org/10.1097/MNM.0000000000000610.

[29] Agool A, Slart RHJA, Dierckx RAJO, Kluin PM, Visser L, Jager PL, et al. Somatostatin receptor scintigraphy might be useful for detecting skeleton abnormalities in patients with multiple myeloma and plasmacytoma. Eur J Nucl Med Mol Imaging. 2010;37:124–30. https://doi.org/10.1007/s00259-009-1199-5.

[30] Kerros C, Cavey T, Sola B, Jauzac P, Allouche S. Somatostatin and opioid receptors do not regulate proliferation or apoptosis of the human multiple myeloma U266 cells. J Exp Clin Cancer Res CR. 2009;28:77. https://doi.org/10.1186/1756-9966-28-77.

[31] Gradiz R, Silva HC, Carvalho L, Botelho MF, Mota-Pinto A. MIA PaCa-2 and PANC-1 - pancreas ductal adenocarcinoma cell lines with neuroendocrine differentiation and somatostatin receptors. Sci Rep. 2016;6:21648. https://doi.org/10.1038/srep21648.

[32] Modarai SR, Opdenaker LM, Viswanathan V, Fields JZ, Boman BM. Somatostatin signaling via SSTR1 contributes to the quiescence of colon cancer stem cells. BMC Cancer. 2016;16. https://doi.org/10.1186/s12885-016-2969-7.

[33] Hill RP. The changing paradigm of tumour response to irradiation. Br J Radiol. 2017;90. https://doi.org/10.1259/bjr.20160474.

[34] Marin G, Vanderlinden B, Karfis I, Guiot T, Wimana Z, Reynaert N, et al. A dosimetry procedure for organs-at-risk in 177Lu peptide receptor radionuclide therapy of patients with neuroendocrine tumours. Phys Medica PM Int J Devoted Appl Phys Med Biol Off J Ital Assoc Biomed Phys AIFB. 2018;56:41–9. https://doi.org/10.1016/j.ejmp.2018.11.001.

[35] Fastrez M, Artigas C, Sirtaine N, Wimana Z, Caillet M, Rozenberg S, et al. Value of the 68Ga-DOTATATE PET-CT in the diagnosis of endometriosis. A pilot study. Eur J Obstet Gynecol Reprod Biol. 2017;212:69–74. https://doi.org/10.1016/j.ejogrb.2017.03.022.

[36] Wang H, Zhang X. ROS reduction does not decrease the anticancer efficacy of X-ray in two breast cancer cell lines. Oxidative Med Cell Longev. 2019;2019. https://doi.org/10.1155/2019/3782074.

[37] Bozkurt MF, Virgolini I, Balogova S, Beheshti M, Rubello D, Decristoforo C, et al. Guideline for PET/CT imaging of neuroendocrine neoplasms with 68 Ga-DOTA-conjugated somatostatin receptor targeting peptides and 18 F–DOPA. Eur J Nucl Med Mol Imaging. 2017;44:1588–601. https://doi.org/10.1007/s00259-017-3728-y.

[38] O'Neill E, Kersemans V, Allen PD, Terry SYA, Torres JB, Mosley M, et al. Imaging DNA damage repair in vivo after 177Lu-DOTATATE therapy. J Nucl Med. 2020;61:743–50. https://doi.org/10.2967/jnumed.119.232934.

[39] Cullinane C, Waldeck K, Kirby L, Rogers BE, Eu P, Tothill RW, et al. Enhancing the anti-tumour activity of 177 Lu-DOTA-octreotate radionuclide therapy in somatostatin receptor-2 expressing tumour models by targeting PARP. Sci Rep. 2020;10:1–10. https://doi.org/10.1038/s41598-020-67199-9.

[40] Sharma R, Wang WM, Yusuf S, Evans J, Ramaswami R, Wernig F, et al. 68Ga-DOTATATE PET/CT parameters predict response to peptide receptor radionuclide therapy in neuroendocrine tumours. Radiother Oncol. 2019;141:108–15. https://doi.org/10.1016/j.radonc.2019.09.003.

[41] Kratochwil C, Stefanova M, Mavriopoulou E, Holland-Letz T, Dimitrakopoulou-Strauss A, Afshar-Oromieh A, et al. SUV of [68Ga]DOTATOC-PET/CT predicts response probability of PRRT in neuroendocrine tumors. Mol Imaging Biol. 2015;17:313–8. https://doi.org/10.1007/s11307-014-0795-3.

[42] Ç S, A P, E Ö, Ön K, Mk K. The role of baseline Ga-68 DOTATATE positron emission tomography/computed tomography in the prediction of response to fixed-dose peptide receptor radionuclide therapy with Lu-177 DOTATATE. Turk J Med Sci. 2016. https://doi.org/10.3906/sag-1412-11.

[43] Öksüz MÖ, Winter L, Pfannenberg C, Reischl G, Müssig K, Bares R, et al. Peptide receptor radionuclide therapy of neuroendocrine tumors with 90Y-DOTATOC: is treatment response predictable by pre-therapeutic uptake of 68Ga-DOTATOC? Diagn Interv Imaging. 2014;95:289–300. https://doi.org/10.1016/j.diii.2013.07.006.

[44] Brunner P, Jörg A-C, Glatz K, Bubendorf L, Radojewski P, Umlauft M, et al. The prognostic and predictive value of sstr2-immunohistochemistry and sstr2-targeted imaging in neuroendocrine tumors. Eur J Nucl Med Mol Imaging. 2017;44:468–75. https://doi.org/10.1007/s00259-016-3486-2.

[45] Bodei L, Kidd MS, Singh A, van der Zwan WA, Severi S, Drozdov IA, et al. PRRT genomic signature in blood for prediction of 177Lu-octreotate efficacy. Eur J Nucl Med Mol Imaging. 2018;45:1155–69. https://doi.org/10.1007/s00259-018-3967-6.

[46] Emmett L, Crumbaker M, Ho B, Willowson K, Eu P, Ratnayake L, et al. Results of a prospective phase 2 pilot trial of 177Lu–PSMA-617 therapy for metastatic castration-resistant prostate cancer including imaging predictors of treatment response and patterns of progression. Clin Genitourin Cancer. 2019;17:15–22. https://doi.org/10.1016/j.clgc.2018.09.014.
[47] Ilan E, Sandström M, Wassberg C, Sundin A, Garske-Román U, Eriksson B, et al. Dose response of pancreatic neuroendocrine tumors treated with peptide receptor radionuclide therapy using 177Lu-DOTATATE. J Nucl Med. 2015;56:177–82. https://doi.org/10.2967/jnumed.114.148437.
[48] Ighodaro OM, Akinloye OA. First line defence antioxidants-superoxide dismutase (SOD), catalase (CAT) and glutathione peroxidase (GPX): their fundamental role in the entire antioxidant defence grid. Alex J Med. 2018;54:287–93. https://doi.org/10.1016/j.ajme.2017.09.001.
[49] Forman HJ, Zhang H, Rinna A. Glutathione: overview of its protective roles, measurement, and biosynthesis. Mol Asp Med. 2009;30:1–12. https://doi.org/10.1016/j.mam.2008.08.006.
[50] Liou G-Y, Storz P. Reactive oxygen species in cancer. Free Radic Res. 2010;44. https://doi.org/10.3109/10715761003667554.
[51] Tang L, Wei F, Wu Y, He Y, Shi L, Xiong F, et al. Role of metabolism in cancer cell radioresistance and radiosensitization methods. J Exp Clin Cancer Res. 2018;37:87. https://doi.org/10.1186/s13046-018-0758-7.
[52] Kirsch DG, Diehn M, Kesarwala AH, Maity A, Morgan MA, Schwarz JK, et al. The future of radiobiology. JNCI J Natl Cancer Inst. 2017;110:329–40. https://doi.org/10.1093/jnci/djx231.
[53] Birben E, Sahiner UM, Sackesen C, Erzurum S, Kalayci O. Oxidative stress and antioxidant defense. World Allergy Organ J. 2012;5:9–19. https://doi.org/10.1097/WOX.0b013e3182439613.
[54] Andrisse S, Koehler RM, Chen JE, Patel GD, Vallurupalli VR, Ratliff BA, et al. Role of GLUT1 in regulation of reactive oxygen species. Redox Biol. 2014;2:764–71. https://doi.org/10.1016/j.redox.2014.03.004.
[55] Giunta S, Belotserkovskaya R, Jackson SP. DNA damage signaling in response to double-strand breaks during mitosis. J Cell Biol. 2010;190:197–207. https://doi.org/10.1083/jcb.200911156.
[56] Nonnekens J, van Kranenburg M, Beerens CEMT, Suker M, Doukas M, van Eijck CHJ, et al. Potentiation of peptide receptor radionuclide therapy by the PARP inhibitor olaparib. Theranostics. 2016;6:1821–32. https://doi.org/10.7150/thno.15311.
[57] Purohit NK, Shah RG, Adant S, Hoepfner M, Shah GM, Beauregard J-M. Potentiation of 177Lu-octreotate peptide receptor radionuclide therapy of human neuroendocrine tumor cells by PARP inhibitor. Oncotarget. 2018;9:24693–706. https://doi.org/10.18632/oncotarget.25266.
[58] Bishay K, Ory K, Olivier M-F, Lebeau J, Levalois C, Chevillard S. DNA damage-related RNA expression to assess individual sensitivity to ionizing radiation. Carcinogenesis. 2001;22:1179–83. https://doi.org/10.1093/carcin/22.8.1179.
[59] Pitroda SP, Pashtan IM, Logan HL, Budke B, Darga TE, Weichselbaum RR, et al. DNA repair pathway gene expression score correlates with repair proficiency and tumor sensitivity to chemotherapy. Sci Transl Med. 2014;6:229ra42. https://doi.org/10.1126/scitranslmed.3008291.
[60] Ledermann JA, Pujade-Lauraine E. Olaparib as maintenance treatment for patients with platinum-sensitive relapsed ovarian cancer. Ther Adv Med Oncol. 2019;11. https://doi.org/10.1177/1758835919849753.
[61] Chavaudra N, Bourhis J, Foray N. Quantified relationship between cellular radiosensitivity, DNA repair defects and chromatin relaxation: a study of 19 human tumour cell lines from different origin. Radiother Oncol. 2004;73:373–82. https://doi.org/10.1016/j.radonc.2004.07.016.
[62] Banáth JP, MacPhail SH, Olive PL. Radiation sensitivity, H2AX phosphorylation, and kinetics of repair of DNA Strand breaks in irradiated cervical cancer cell lines. Cancer Res. 2004;64:7144–9. https://doi.org/10.1158/0008-5472.CAN-04-1433.
[63] Wu Y, Pfeifer AK, Myschetzky R, Garbyal RS, Rasmussen P, Knigge U, et al. Induction of anti-tumor immune responses by peptide receptor radionuclide therapy with 177Lu-DOTATATE in a murine model of a human neuroendocrine tumor. Diagnostics. 2013;3:344–55. https://doi.org/10.3390/diagnostics3040344.
[64] Kidd M, Modlin IM. The role of liquid biopsies to manage and predict PRRT for NETs. Nat Rev Gastroenterol Hepatol. 2017;14:331–2. https://doi.org/10.1038/nrgastro.2017.26.
[65] Bodei L, Schöder H, Baum RP, Herrmann K, Strosberg J, Caplin M, et al. Molecular profiling of neuroendocrine tumours to predict response and toxicity to peptide receptor radionuclide therapy. Lancet Oncol. 2020;21:e431–43. https://doi.org/10.1016/S1470-2045(20)30323-5.
[66] Terry SYA, Nonnekens J, Aerts A, Baatout S, de Jong M, Cornelissen B, et al. Call to arms: need for radiobiology in molecular radionuclide therapy. Eur J Nucl Med Mol Imaging. 2019;46:1588–90. https://doi.org/10.1007/s00259-019-04334-3.